HYDROLOGICAL PROCESSES
Hydrol. Process. (2015)
Published online in Wiley Online Library
(wileyonlinelibrary.com) DOI: 10.1002/hyp.10450

Climate warming causes intensification of the hydrological cycle, resulting in changes to the vernal and autumnal windows in a northern temperate forest

I. F. Creed,[1]* T. Hwang,[2] B. Lutz[3] and D. Way[1,4]

[1] *Department of Biology, Western University, 1151 Richmond Street, London, Ontario, N6A 5B7, Canada*
[2] *Department of Geography, Indiana University, Bloomington, IN, 47405, USA*
[3] *Department of Biological Sciences, Center for Ecology and Natural Resources Sustainability, Kent State University, 256 Cunningham Hall, Kent, OH, 44242, USA*
[4] *Nicholas School of the Environment, Duke University, Durham, NC 27708, USA*

Abstract:

Climate warming is likely to lead to complex effects on northern forests of the temperate forest biome. We investigated whether rising temperatures altered the timing of snowmelt and snowpack accumulation or extended the forest growing season length in the Turkey Lakes Watershed in central Ontario. Archived satellite imagery was used to track changes in timing of snowpack loss/gain and canopy leaf on/off; the periods between these events were defined as the vernal (spring) and autumnal (fall) windows. We found only a slight extension of the growing season into the autumn period and no increase in the width of the vernal or autumnal windows, indicating that forest growth is not responding significantly to temperature increases during these windows. Archived time series of temperature, precipitation and discharge data for a nested set of catchments ranging in size from headwater (<10 ha) to regional (10^3 ha) catchments were used to track changes in the magnitude, timing and partitioning of precipitation into evapotranspiration and discharge. We found an intensification of hydrological cycling, with (1) a higher dryness index (PET/P) during the summer growing season and (2) earlier spring snowmelt discharges, and later more concentrated autumn storm discharges during the shoulder seasons. This intensification of the hydrological cycle during the summer growth season and the vernal and autumnal windows may not only limit opportunities for enhanced forest growth, but may be contributing to the recent observations of forest decline within this biome. Copyright © 2015 John Wiley & Sons, Ltd.

KEY WORDS climate; temperate; forest; phenology; hydrological intensification

Received 14 April 2014; Accepted 26 January 2015

INTRODUCTION

Evidence of global scale climate warming is now overwhelming (Jansen and Overpeck, 2007), and most forecasts predict increasing temperatures and associated changes to the hydrological cycle resulting in increased frequency of extreme weather events (Katz and Brown, 1992; Beniston *et al*., 2007; Capell *et al*., 2014). In forests, photosynthesis, carbon and water cycling are interrelated, as CO_2 uptake and evaporative water loss are inherently linked through stomata. Forest water-use efficiency, which measures the amount of carbon fixed per unit of water lost (Cowan and Farquhar, 1977), is relatively constant in northern forests (e.g. Brummer *et al.*, 2012). However, the response of mid-to-high latitude forest processes to climate change is expected to be complex, as forest growth and associated water use are functions of many different drivers, including photoperiod, light, energy, water and nutrient availability (Boisvenue and Running, 2006), and climate warming may disrupt existing relationships among these drivers.

Northern forests may respond to different cues as the climate changes (Bauerle *et al.*, 2012; Rustad *et al.,* 2012). Climate warming may extend the growing season of forests if temperature cues regulate the timing of canopy development, but only if tree phenology is mostly responsive to spring and autumn temperatures, rather than photoperiod cues and chilling requirements (Zhang *et al.*, 2007; Morisette *et al.,* 2008; Way, 2011b; Bauerle *et al.*, 2012). In temperate forest biomes, forest carbon uptake capacity is more tightly correlated with day length than temperature (Bauerle *et al.*, 2012), suggesting that climate warming will not extend the period of forest carbon uptake in a simplistic manner (Stoy *et al*., 2014). In contrast, the forest hydrological cycle responds to temperature, although the hydrological response of

*Correspondence to: Irena F. Creed, Department of Biology, Western University, London, Ontario, Canada, N6A 5B7.
E-mail: icreed@uwo.ca

northern forests to climate warming is variable across different forest types (Jones *et al.*, 2012). For example, annual water yields from coniferous and deciduous forests seem less resilient to climate warming than mixed forests (Creed *et al.*, 2014). Furthermore, climate warming, or climate driven warming of the global land surface and lower atmosphere, may result in intensification of the global hydrological cycle, with a warmer atmosphere able to absorb more water (i.e. higher evapotranspiration) and transport this water elsewhere, resulting in changes to water yields (Durack *et al.*, 2012), with wet areas becoming wetter and dry areas becoming drier, relative to global means (Chou *et al.*, 2009). This hydrological intensification may lead to more frequent and extreme hydrological events, such as storms, floods and droughts. The different drivers of physiological and hydrological processes in forests are likely to lead to fundamental changes in these ecosystems, especially if the seasonal timing of these drivers responds differently to climate change.

Declines in annual water yields have been observed in temperate forest biomes (e.g. Mengistu *et al.*, 2013). However, more information is needed about the timing and magnitude of this decline, providing insight into the potential for hydrological extremes, i.e. floods and droughts (Lehner *et al.*, 2006), changes in biogeochemical nutrient export, consequences for downstream productivity and diversity of aquatic ecosystems (Mengistu *et al.*, 2013). In particular, data are needed on hydrological changes during the critical shoulder seasons of forest growth in deciduous forests, the vernal and autumnal periods, when the majority of water flows off forest landscapes. Grime (1994) coined the term 'vernal window' in reference to the period of high irradiance on the forest floor under an open canopy, which causes a surge in productivity of the understory in the spring. Tockner *et al.* (2010) extended this concept to discuss a vernal and autumnal window of 'ecological opportunity', albeit in aquatic ecosystems, where they observed a spike in invertebrate and phytoplankton growth in riverine floodplains. There is a need to consider the hydrological controls on these windows of ecological opportunities; for example, if hydrological flows decline in magnitude and shift their timing, this may lead to feedbacks resulting in fundamental ecological changes on the forest landscape (e.g. Hu *et al.*, 2010).

The purpose of this paper was to explore the effects of climate warming on the hydrology and ecology of the northern limits of the temperate forest biome, particularly focusing on hydrological changes within the vernal and autumnal windows. We defined the vernal window as the time period between the end of snowpack and beginning of canopy leaf flush in spring, and the autumnal window as the time period between the end of canopy leaf fall and start of snowpack in autumn. We hypothesized that climate warming is leading to a temperature-driven widening of both the vernal and autumnal windows, and that an intensification of the hydrological cycle during these windows limits opportunities for forest growth. We tested these hypotheses by tracking changes in the partitioning of water flows into the atmosphere (evapotranspiration) or aquatic ecosystems (discharge) and changes in the timing of forest canopy and snowpack presence on a temperate forest landscape, and pose the following questions:

1. Is the timing of forest growth in a temperature-limited northern forest expanding into the vernal and autumnal windows as the climate warms?
2. Are changes in the hydrological cycle leading to an earlier end to snowmelt and later onset of autumn storms during the vernal and autumnal windows, respectively?
3. Are changes in phenological and hydrological processes affected by climate warming equally, or has recent warming induced a mismatch, whereby forest leaf emergence and tree water availability are uncoupled from their previous relationship?

We posed these questions for a temperate forest of the Great Lakes – St Lawrence River forest region over an almost 30-year warming trajectory and discuss potential implications of this climate change on the primary productivity of both terrestrial and aquatic ecosystems on forested landscapes.

STUDY AREA

The Batchawana River Watershed (1280 km^2) drains into Batchawana Bay on the eastern shoreline of Lake Superior in central Ontario, Canada. The Turkey Lakes Watershed (TLW) is a 10.5 km^2 subwatershed that drains into the lower reaches of Batchawana River through Norberg Creek (Figure 1). The TLW is a temperate forest in one of the largest areas of forested landscapes remaining in the Laurentian Great Lakes basin. The forest is an old growth stand of shade-tolerant hardwood species dominated by sugar maple.

Within the TLW, the climate is continental with precipitation driven by lake effect precipitation from Lake Superior and local orographic effects in areas of high relief, particularly Batchawana Mountain (664 m), one of the highest elevation peaks in Ontario, Canada. From 1981 to 2009, the average annual (calendar year) precipitation was 1195 mm and average annual temperature was 4.6 °C. The frost-free period in the TLW normally extends from May to September, and the

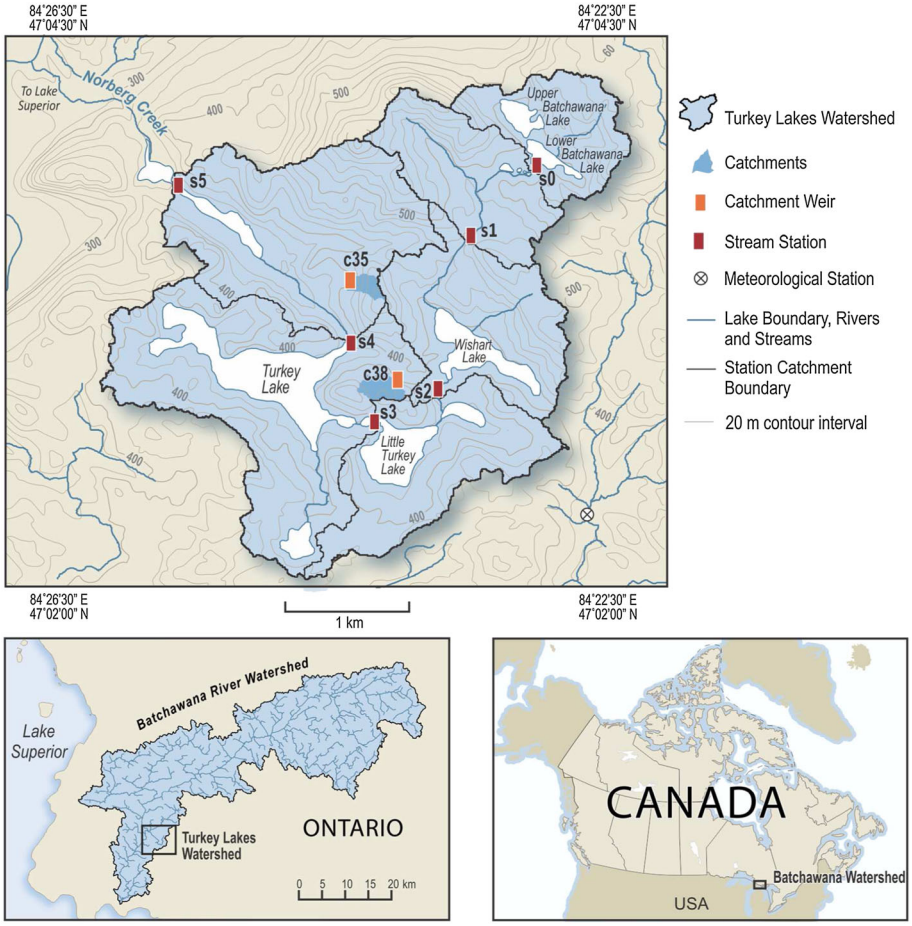

Figure 1. Study area map of the Turkey Lakes Watershed located within the Batchawana River Watershed in central Ontario

majority of precipitation falls from August to December as rain and snow. A snowpack persists from late November or early December through late March or early April, and peak stream discharge occurs during spring snowmelt and again during autumn storms. The overall relief is 400 m (664 to 264 m). Bedrock is Precambrian silicate greenstone formed from metamorphosed basalt, with small outcrops of felsic igneous rock (Semkin and Jeffries, 1983). Overlying the bedrock is a thin and discontinuous till, ranging in depth from <1 m at higher elevations (with infrequent surface exposure of bedrock) to 1–2 m at lower elevations, although till deposits of up to 65 m occasionally occur in bedrock depressions (Elliot, 1985). The till is double-layered, comprising a thin permeable (saturated hydraulic conductivity of 10^{-3} cm/s) sandy loam ablation till overlying a thicker, less permeable (saturated hydraulic conductivity of 10^{-5} cm/s) silt loam basal till (Craig and Johnston, 1988). The podzolic soils that have developed in the till follow a generalized sequence of thin and undifferentiated near the ridge, gradually thickening, differentiating and increasing in organic content on topographic benches and towards the stream (Creed *et al.*, 2002). Highly humified organic deposits occur in wetlands (Wickware and Cowell, 1985).

The TLW has been monitored by federal government agencies since 1980 to assess the potential impacts of acid rain and climate change on terrestrial and aquatic ecosystems (*cf.* Jeffries *et al.*, 1988). This study focuses on changes in hydrological cycling estimated from a nested set of catchments, including headwater catchments representative of the extremes in percentage of wetlands within the watershed (c38 and c35), and a series of catchments flowing through a chain of lakes to the outflow of the TLW at Norberg Creek (s0 to s5). We used data collected during the 27-year period from 1983 to 2009 as the basis of our analyses.

The chain of catchments ranged from small headwater systems (c38 and c35) through a nested chain of lake outflows (s0 to s5) with catchment areas ranging from 10^0 to 10^3 ha. Slopes ranged from 10° to 20°, and aspect was variable, ranging from N–NE–E to W–SW. The percentage of wetlands had the greatest variability in headwater systems and ranged from 1.1% to 20.5%, while the

percentage of wetlands and lakes in catchments downstream contributing to lake outflows showed less variability and ranged from 13.9% to 20.0% (Table I).

METHODS

Characterizing headwater and regional catchments

Digital terrain analysis using a 5 m digital elevation model from Light Detection and Ranging (LiDAR) data was used to extract catchments from weir locations and to derive topographic features (*cf.* Creed and Beall, 2009), with a vertical accuracy of 0.15 m in open canopy and 0.30 m under closed canopy. Pits and depression were filled (Planchon and Darboux, 2001), and catchment and contributing areas were determined using the D8 algorithm based on a grid map from weir coordinates (O'Callaghan and Mark, 1984; Jenson and Domingue, 1988). Specific contributing areas and stream lengths were corroborated using field observations of drainage networks. Wetlands were identified using a probabilistic approach (Lindsay and Creed, 2005). Monte Carlo simulations were used to determine the probability of a depression, and a critical threshold of 0.30 (selected by comparison with ground surveyed surface saturated areas, Creed and Beall, 2009) was used with different elevation error terms until a stable solution was identified.

Vernal and autumnal windows

The timing of vernal and autumnal windows was determined using satellite-based estimates of the end of snowpack and start of leaf greening in spring as well as leaf senescence and the start of snowpack formation in autumn from 1983 to 2009. For canopy phenology, we used the Normalized Difference Vegetation Index (NDVI), which is the normalized ratio between surface reflectance in the red and near-infrared portions of the electromagnetic spectrum useful for detecting vegetation phenological changes by characterizing the intensity of photosynthetic activity (Rouse *et al.*, 1973). We recognized that the NDVI detects changes in colour associated with leaf senescence rather than litter fall in deciduous forests (Hwang *et al.*, 2014), and therefore assumed that the timespan between changes in leaf colour and leaf fall are constant with climate warming. Annual growing season length was determined using 8-km grid NDVI data from the Global Inventory Modeling and Mapping Studies (GIMMS) NDVI3g data (Zhu *et al.*, 2013) derived from Advanced Very High Resolution Radiometer (AVHRR) satellite data (provided bimonthly). These data were corrected for sensor calibration, view geometry, volcanic aerosols and other effects not related to vegetation change (Tucker *et al.*, 2005; Carroll *et al.*, 2006). A difference logistic function (Fisher *et al.*, 2006) was used to fit the time series of NDVI data (y) each year as a function of day of year (DOY; t) (Figure 2):

$$y(t) = \left(\frac{1}{1+e^{a+bt}} - \frac{1}{1+e^{a'+b't}}\right) c + d \qquad (1)$$

where the fitted parameters a and b describe the greenup period, a' and b' for the senescence period, d is the minimum NDVI value, and c is the difference between maximum and minimum NDVI values. The beginning and end of the growing season for each year were defined as the inflexion points of the difference logistic function. These inflexion points have been widely used with remote sensing data to find the steepest points during vegetation transition periods (e.g. Zhang *et al.,* 2004). We used good values in the quality flag (1 or 2) from the original data, which were further processed with a simple two-step filtering method (refer to Hwang *et al.,* 2011a; 2011b for details about filtering and non-linear fitting processes of NDVI data). Deciduous tree phenology derived from GIMMS NDVI by Hwang *et al.* (2014) showed comparable patterns in time with moderate resolution imaging spectroradiometer (MODIS)-derived and plot-observed data with consistent offsets in southern Appalachians. We applied the same technique for this study in the TLW.

For snowpack duration, we used 25-km scale binary snow cover data from National Aeronautics and Space Administration's Northern Hemisphere EASE-Grid 2.0 Weekly Snow Cover and Sea Ice Extent dataset (version 4), which is derived from AVHRR, Geostationary Operational Environmental Satellite and other visible-band meteorological satellite data (Brodzik and Armstrong, 2013). The same difference logistic function (Fisher *et al.*, 2006) was used to fit weekly snow cover grid data for each year (Figure 2). Snowpack duration and

Table I. Properties of catchments in the Turkey Lakes Watershed (c38 and c35), as well as a series of streams flowing through a chain of lakes to the outflow of the Turkey Lakes Watershed at Norberg Creek (s0–s5)

Code	Area (ha)	Mean slope (°)	Mean aspect	Elevation at outflow (m)	Percent wetlands or lakes
c38	6.5	13.5	NE	404.1	20.5
c35	4.0	19.2	W	381.4	1.1
s0	89.1	11.9	NE	495.9	20.0
s1	203.6	12.8	E	446.9	13.9
s2	358.1	12.7	SW	378.0	14.2
s3	507.6	10.0	N	370.5	16.3
s4	810.4	11.2	N	367.7	19.5
s5	1049.6	15.3	SW	338.3	15.9

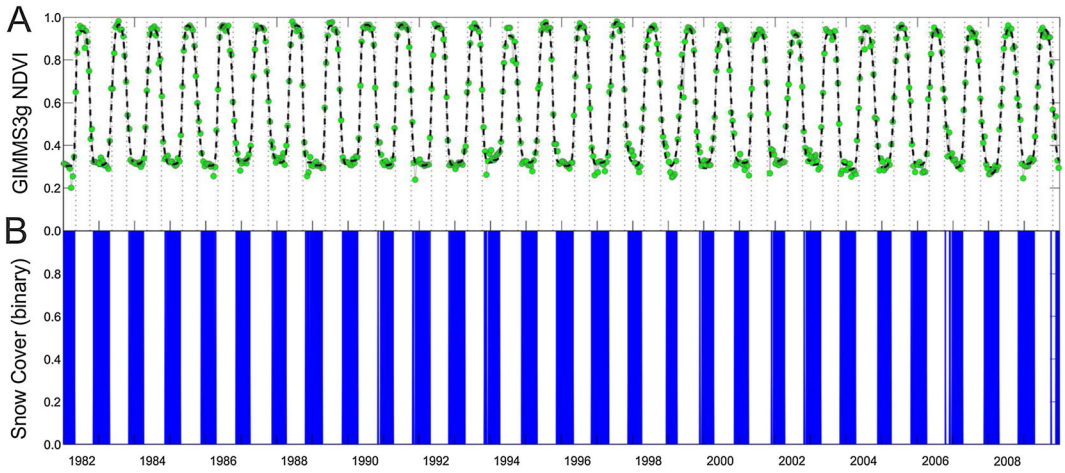

Figure 2. Time series of (A) bimonthly GIMMS3g Normalized Difference Vegetation Index (NDVI) values (green symbols) and fitted logistic functions (dashed lines) and (B) binary weekly snowpack data at the study site during the period from 1982 to 2009. Vertical lines represent the inflexion points of the difference logistic function, used as greenup and senescence timing in this study

the timing of snowpack disappearance in spring and appearance in autumn for each year were defined as the inflexion points of the difference logistic function. Site-based data were used as a cross-reference, although ground-truthed 'snow off' data were more precise than 'snow on' data (R. G. Semkin, Environment Canada; Unpublished data; Data not shown). All non-linear regressions were performed using iterative least squares estimation with the *nlinfit* function in MATLAB [The Mathworks Inc., Torrance, CA, USA, which uses the Levenburg–Marquardt algorithm (Marquardt, 1963)].

Intensification of hydrological cycle

The intensification of hydrological cycling was investigated using estimates of precipitation partitioning between evapotranspiration (ET) *versus* discharge (Q), and the timing and duration of water flows during spring melt and autumn storms during the time series from 1983 to 2009. Daily meteorological data were obtained from the Canadian Air and Precipitation Monitoring Network meteorological station located just outside the TLW (latitude 47°02°06°N; longitude 84°22°52°W). Daily discharge data for two headwater catchments (c38 and c35) were collected from sampling stations in the TLW (data from F. D. Beall, Great Lakes Forestry Centre (GLFC), Sault Ste. Marie, Ontario, Canada). Daily discharge data for catchments draining through the headwater chain of lakes to the TLW outlet at Norberg Creek were downloaded from the Water Survey of Canada's HYDAT database (Environment Canada, 2014).

We examined these data for trends in annual, monthly and daily time series. For *annual* data, we applied a simple linear regression model to detect significant annual trends in temperature (T), precipitation (P) and Q. For *monthly* data, we examined trends in T and P, and used the Budyko (1974) dryness index (the ratio of potential evapotranspiration to precipitation, PET/P) and evaporative index [(P−Q)/P] to explore changes in hydrologic dynamics within the forested catchments. We were unable to account for storage at the monthly scale, so we call it the 'evaporative-storage' index. We calculated PET from mean monthly T values using the method of Hamon (1963). While the Hamon (1963) method may underestimate PET, it performs better than other T-based PET models and about the same as radiation-based PET models (Lu *et al.*, 2005). We then applied a Seasonal Trend decomposition using Loess (STL) algorithm (Cleveland *et al.*, 1990) to determine the monthly trends for P and T for the TLW, and the monthly trends for PET/P and (P−Q)/P for each of the study catchments. STL filters time series data into long-term (i.e. inter-annual), monthly and residual components using Loess smoothing, which allowed for robust estimates of monthly trends without distortion from long-term trends and atypical data behaviour (Cleveland *et al.*, 1990).

For *daily* data, to analyse long-term trends in precipitation and streamflow timing, we partitioned each year into two six-month periods to account for the two periods during which the majority of discharge flows from the landscape: the first dominated by snowmelt (January to June) and the second by late summer/early fall rains (July to December). For each period, the 50th percentiles of cumulative precipitation and stream discharge were calculated to estimate centre of mass, the 10th, 20th and 25th percentiles were calculated to characterize changes to the beginning of the two hydrographs, and the 75th, 80th and 90th percentiles were calculated to characterize changes at the end of the two hydrographs. Changes in

the day of year when these percentiles were attained for each period over the years showed whether the timing of water flux was changing (i.e. shifting to earlier or later dates). For each period, the number of days over which a specific range in percentiles of water flux occurred was also calculated (i.e. 10th to 90th, 20th to 80th, or 25th to 75th percentiles). Changes in the number of days over which the majority of precipitation or discharge occurred showed whether the shape of the hydrograph was changing (i.e. sharpening or flattening). Trends in precipitation and discharge timing were analysed for each catchment using Mann–Kendall and Theil–Sen analysis for monotonic trends in hydrological data (Sen, 1968; Yue *et al.*, 2002) using the 'zyp' and 'Kendall' packages in *R* (v.3.0.2). Autocorrelation in hydrological data was corrected for using the Zhang prewhitening method (Zhang *et al.*, 2000), where significant trends were detected and removed from the time series, autocorrelation computed, and this process was repeated until differences in estimates of slope and the auto-regressive model were less than 1% in two consecutive iterations. The Mann–Kendall test for trends was then used on the resultant hydrological data, and the Theil–Sen test was used to calculate the slope of the trend (Sen, 1968), and the intercepts were calculated as the median of the intercepts. We used a value of $P < 0.05$ to detect significant trends and $P < 0.1$ to suggest trends. Outliers were removed using Cook's Distance (D) measurements, where outliers were identified as $D \geq 4/N$ where N is the number of observations ($N = 27$ from 1983 to 2009).

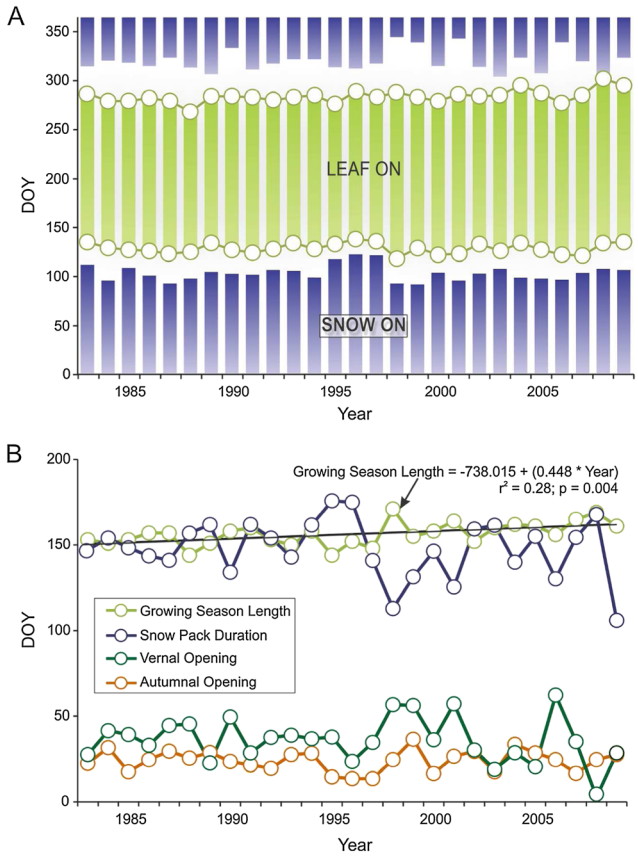

Figure 3. (**A**) Time series of yearly timing of snow cover (purple bars), canopy leaf cover (green bars) and vernal and autumnal windows (spaces between) in the Turkey Lakes Watershed and (**B**) time series of the length in days of growing season (green circles), snowpack (purple circles) and vernal (dark green) and autumnal (orange) windows. DOY, day of year

RESULTS

Evidence of widening of vernal or autumnal windows

Satellite-based evidence showing the changes in the vernal or autumnal windows is presented in Figure 2. The spring end of snowpack ranged from calendar day of year 92 (April 2) to year 124 (May 3) and the autumn start of snowpack ranged from calendar day of year 304 (October 31) to year 345 (December 11) (Figure 3). Despite this broad range in dates, no significant trends in snow off or snow on dates were found over the time series ($P > 0.1$). The spring start of canopy greening ranged from calendar day of year 117 (April 27) to year 137 (May 17), and the autumn end of canopy senescence ranged from calendar day of year 268 (September 25) to year 302 (October 28). No significant trends in the timing of canopy greening were found over the time series, while growing season length significantly increased during the same period, mostly driven by delayed timing of canopy senescence ($P < 0.05$). The vernal window, defined as the period from the disappearance of the snowpack to the development of the forest canopy ranged from 8 to 37 days, and the autumnal window from canopy senescence to snowpack appearance ranged from 3 to 62 days. Despite the extension in growing season length and associated shift in the autumnal window, there was no statistically significant widening (or narrowing) of the windows over the time series based on remote sensing data (Figure 3). However, it is worthwhile to note that the vernal window shows a nonsignificant increase over the time series, while the autumnal window shows a nonsignificant decrease.

Evidence for intensification of hydrological cycle

a) Annual changes

There was a significant increase in mean annual air temperature (calendar year) of 0.6 °C per decade ($P = 0.02$). This warming was related to changes in hydrological cycles, as evidenced by declines in total annual precipitation at a rate of 82.2 mm per decade ($P = 0.03$) and total annual discharge at a rate of 109.6 mm per decade ($P < 0.01$) (Figure 4).

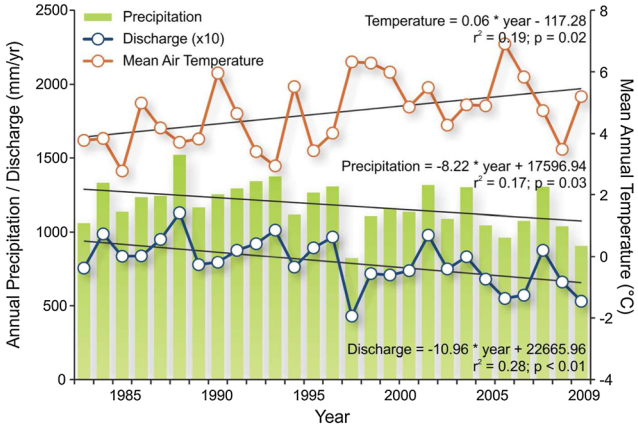

Figure 4. Annual time series of precipitation (green bars) and temperature (orange circles) collected from the Canadian Air and Precipitation Monitoring Network's meteorological station located just outside of the Turkey Lakes Watershed and discharge (blue circles) from the s5 weir that drains the Turkey Lakes Watershed at Norberg Creek

b) Seasonal changes

No change was found in the seasonality of temperature, suggesting that the warming we observe at the annual scale is occurring in all months, but a change in seasonality was found in precipitation, particularly in the autumn (Figure 5). This late season change in precipitation was characterized by decreasing precipitation in August and September and increasing precipitation in October over the time series (Figure 5).

With respect to the dryness and evaporative-storage indices, PET/P decreased (i.e. relative to a given amount of P, PET decreased and sites became wetter) over the time series in all months except for May, June, July and August, when it increased (i.e. relative to a given amount of P, PET increased and sites became drier) (Figure 6). In spring, (P−Q)/P decreased (i.e. relatively more Q) in March and April over the time series, but increased (i.e. relatively less Q) in May over the time series, suggesting a shift in snow storage and a shift to earlier snowmelts (Figure 6). The signal may have been intensifying downstream; namely, there was a weak signal in headwater catchments that appeared to strengthen downstream (Figure 6). The weaker signal in headwater catchments may have been due to the fact that these headwater catchments showed different responses depending on the proportion of wetland features. The headwater catchment with substantial surface water storage potential (c38, with 20.5% wetland) showed an increase in (P−Q)/P during the spring snowmelt period over the time series. In contrast, the headwater catchment with minimal water storage potential (c35, with only 1.1% wetland) showed a decrease in (P−Q)/P during the spring snowmelt period over the time series (Figure 6). In autumn, (P−Q)/P increased (i.e. less Q) in September and October, but not in November or December, with this signal also appearing to intensify downstream over the time series (Figure 6).

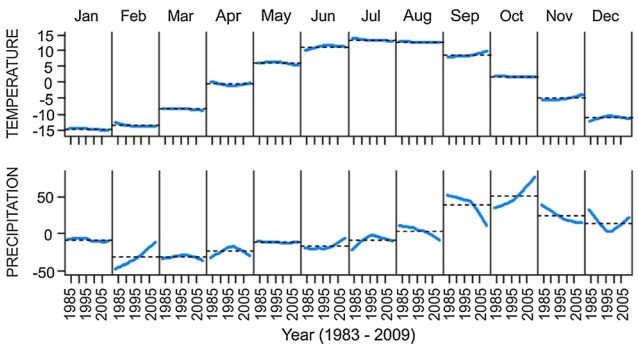

Figure 5. Monthly time series of temperature and precipitation from 1983 to 2009 with inter-annual trends removed

c) Daily changes

Two potential changes were examined during the two major discharge periods captured in the January-to-June and the July-to-December periods: (1) a shift in the timing of water flux to earlier (left) or later (right) in the year, as indicated by either a negative or positive, respectively, Theil–Sen Slope for the day-of-year of different percentiles (10th, 20th, 25th, 50th, 75th, 80th and 90th) over the observed period and (2) a change in the duration of discharge reflecting either a flattening or peaking of water flux as indicated by a positive or negative, respectively, Theil–Sen slope relationship between the number of days of different percentile ranges (10th to 90th, 20th to 80th and 25th to 75th) and year. Details of the statistical results indicating which changes in timing and duration were significant in the headwater catchments are provided in Table II, with the pattern of changes in P in Table III and for Q in the headwater and downstream catchments in Table IV. In general, we observed similar patterns when analysing data with and without outliers identified through Cook's Distance analysis.

For the spring and fall frequency distributions of daily precipitation that fell from January to June and July to December (Table IIA), significant trends in the timing of the 20th and 25th percentiles of spring precipitation were observed using Mann–Kendall tests; however, the median slopes as calculated by Theil–Sen analysis were zero in both cases. The trends of these differences are summarized in Table III. We observed a significant change in the duration (i.e. number of days) of the 20th to 80th percentile range during the autumn, which shrank by 1.8 days over the course of the 27 years we investigated.

For the spring frequency distribution of daily discharge that fell during the period from January to June (Table IIB, Table IV), there were significant shifts in the timing of percentiles to an earlier day of year (i.e. left arrows) indicating shifts to an earlier end of spring discharge. For

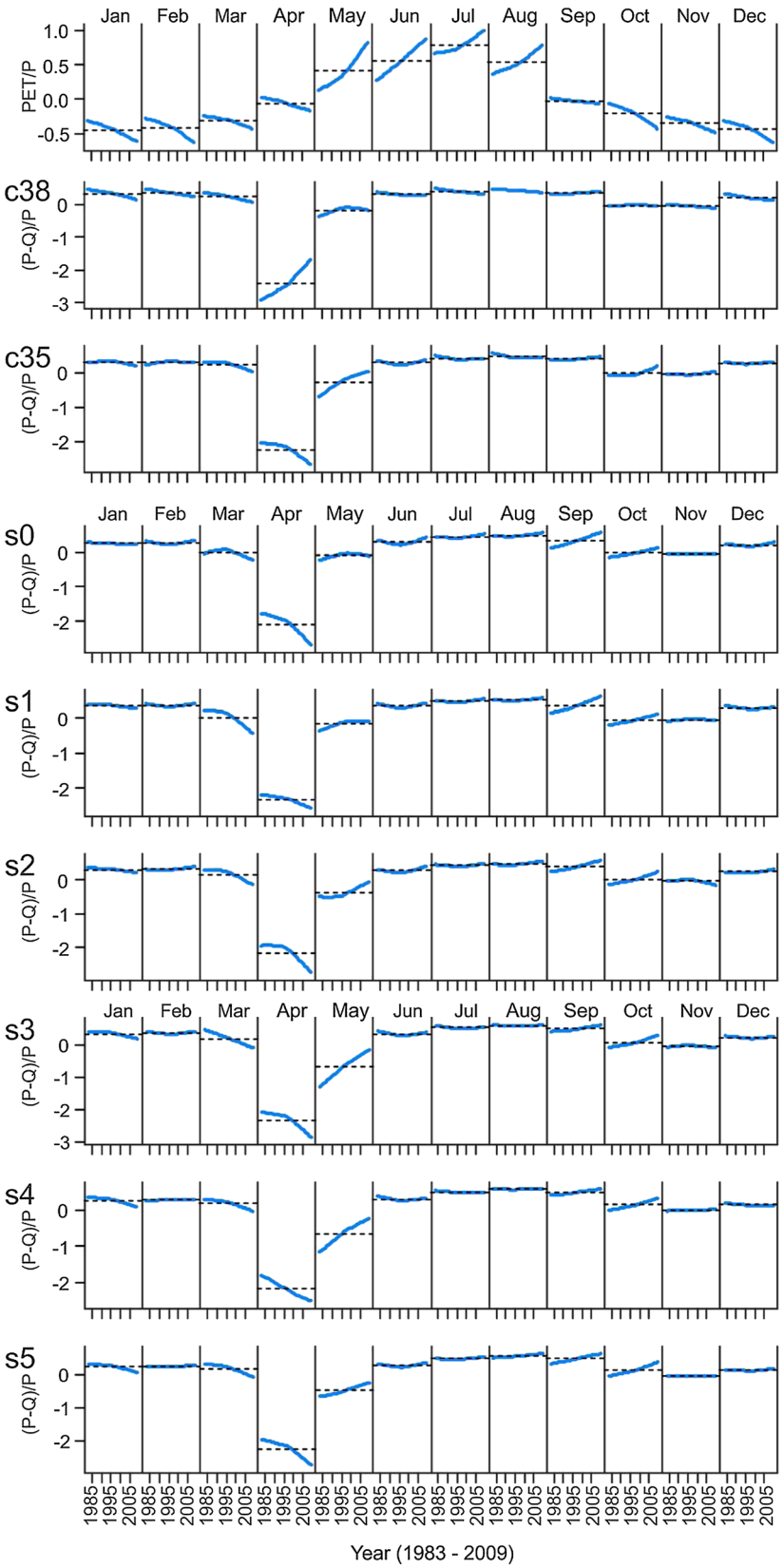

Figure 6. Monthly time series from 1983 to 2009 of dryness index [potential evapotranspiration (PET)/precipitation (P)] from the meteorological station and evaporative-storage index [(P−Q)/P] from catchments of the Turkey Lakes Watershed (c38 and c35) and a series of streams flowing through a chain of lakes to the outflow of the Turkey Lakes Watershed (s0–s5) with the inter-annual trends removed

Table II. Results of Mann–Kendall and Theil–Sen analysis on frequency distributions of spring and autumn precipitation, c38 discharge and c35 discharge from 1983 to 2009 showing shifts in the timing of the 10th, 20th, 25th, 50th, 75th, 80th and 90th percentiles and changes in duration in the ranges of the 10th to 90th, 20th to 80th and 25th to 75th percentiles. Positive Theil–Sen slope Δ/Year values indicate shifts to later in the year (timing) and increases in range over time (duration), and negative Theil–Sen slope Δ/Year values indicate shifts to earlier in the year (timing) and decreases in range over time (duration). Bolded rows indicate $P < 0.1$ with Theil–Sen slopes greater than zero

2A: Precipitation

Timing of precipitation

Spring

Percentile	Theil–Sen Slope Δ per decade (days)	Theil–Sen Slope (days)	Mann–Kendall τ	Mann–Kendall *P*	Auto-correlation	Intercept
10	0.00	0.00	0.198	0.211	−0.349	19.000
20	0.00	0.00	−0.350	0.031	−0.340	37.000
25	0.00	0.00	0.365	0.015	−0.074	46.000
50	0.00	0.00	0.245	0.109	−0.240	91.000
75	0.00	0.00	0.133	0.407	0.115	136.000
80	0.00	0.00	−0.056	0.727	−0.046	144.500
90	0.00	0.00	−0.105	0.499	0.071	163.000

Autumn

10	0.00	0.00	0.227	0.166	−0.170	201.000
20	0.00	0.00	0.239	0.127	0.225	219.000
25	0.00	0.00	−0.044	0.803	0.037	228.000
50	0.00	0.00	0.064	0.696	−0.084	273.000
75	0.00	0.00	0.028	0.885	−0.217	318.000
80	0.00	0.00	−0.255	0.170	−0.056	327.000
90	0.00	0.00	0.137	0.490	0.000	345.000

Duration of Precipitation

Spring

Percentile Range	Theil–Sen Slope Δ per decade (days)	Theil–Sen Slope (days)	Mann–Kendall τ	Mann–Kendall *P*	Auto-correlation	Intercept
10–90	0.00	0.00	−0.083	0.611	0.071	144.000
20–80	**0.00**	**0.00**	**0.112**	**0.495**	**−0.174**	**108.000**
25–75	0.00	0.00	0.036	0.853	−0.260	90.000

Autumn

10–90	0.00	0.00	−0.090	0.619	−0.185	144.000
20–80	**−0.67**	**−1.80**	**−0.297**	**0.064**	**0.110**	**109.200**
25–75	0.00	0.00	0.249	0.127	0.131	90.000

2B: c38 and c35 discharge

Timing of c38 Discharge

Spring

Percentile	Theil–Sen Slope Δ per decade (days)	Theil–Sen Slope (days)	Mann–Kendall τ	Mann–Kendall *P*	Auto-correlation	Intercept
10	**−1.00**	**−27.00**	**−0.366**	**0.009**	**−0.195**	**94.000**
20	−1.91	−5.14	−0.132	0.355	−0.042	100.191
25	−1.77	−4.77	−0.089	0.537	0.026	104.706
50	−2.22	−6.00	−0.028	0.860	0.392	113.667
75	−3.08	−8.31	−0.065	0.659	0.384	123.462
80	−3.33	−9.00	−0.132	0.355	0.043	128.000
90	−4.62	−12.46	−0.163	0.252	−0.227	143.000

Autumn

10	8.57	23.14	0.139	0.332	0.198	255.000
20	8.75	23.63	0.203	0.152	−0.212	269.625
25	7.14	19.29	0.182	0.201	−0.218	274.714
50	4.62	12.46	0.194	0.172	−0.048	296.231
75	**5.71**	**15.43**	**0.372**	**0.008**	**−0.283**	**321.429**
80	**6.43**	**17.36**	**0.342**	**0.015**	**−0.270**	**321.214**

(Continues)

Table II. (*Continued*)

2B: c38 and c35 discharge

90	**4.67**	**12.60**	**0.335**	**0.017**	**−0.310**	**333.400**
		Duration of c38 Discharge				
		Spring				
Percentile Range	Theil–Sen Slope Δ per decade (days)	Theil–Sen Slope (days)	Mann–Kendall τ	Mann–Kendall *P*	Auto-correlation	Interce pt
10–90	**8.57**	**23.14**	**0.286**	**0.043**	**−0.419**	**44.857**
20–80	0.00	0.00	0.040	0.791	−0.325	26.000
25–75	−1.25	−3.38	−0.099	0.494	−0.317	19.625
		Autumn				
10–90	−6.25	−16.88	−0.071	0.628	0.084	88.500
20–80	0.00	0.00	−0.095	0.509	−0.204	52.000
25–75	0.11	3.00	−0.028	0.860	−0.186	40.111
		Timing of c35 Discharge				
		Spring				
Percentile	Theil–Sen Slope Δ/Year	Theil–Sen Slope	Mann–Kendall τ	Mann–Kendall *P*	Auto–correlation	Interce pt
10	0.93	2.501	0.028	0.874	0.331	81.055
20	1.67	4.500	0.027	0.870	−0.160	92.417
25	0.00	0.000	0.000	1.000	−0.097	98.000
50	−1.11	−3.000	−0.037	0.808	0.254	112.333
75	−5.56	−15.000	−0.200	0.168	0.293	125.111
80	**−5.56**	**−15.000**	**−0.283**	**0.056**	**0.205**	**127.111**
90	**−9.47**	**−25.579**	**−0.410**	**0.005**	**−0.253**	**150.132**
		Autumn				
10	**17.78**	**48.000**	**0.267**	**0.065**	**0.083**	**246.389**
20	**8.96**	**24.184**	**0.284**	**0.086**	**0.191**	**273.074**
25	**10.00**	**27.000**	**0.325**	**0.037**	**0.125**	**275.000**
50	4.81	12.981	0.160	0.310	−0.019	293.423
75	1.77	4.781	0.123	0.428	0.084	323.406
80	0.00	0.000	0.115	0.460	0.106	328.000
90	−1.94	−5.250	−0.036	0.833	0.102	343.944
		Duration of c35 Discharge				
		Spring				
Percentile Range	Theil–Sen Slope Δ/Year	Theil–Sen Slope	Mann–Kendall τ	Mann–Kendall *P*	Auto-correlation	Interce pt
10–90	−3.75	−10.125	−0.033	0.834	0.008	71.500
20–80	**−5.00**	**−13.500**	**−0.387**	**0.007**	**−0.385**	**31.500**
25–75	**−3.96**	**−10.683**	**−0.352**	**0.027**	**−0.363**	**23.978**
		Autumn				
10–90	**−20.95**	**−56.571**	**−0.260**	**0.072**	**0.071**	**99.214**
20–80	**−10.00**	**−27.000**	**−0.304**	**0.040**	**0.132**	**57.500**
25–75	**−10.00**	**−27.000**	**−0.355**	**0.016**	**0.143**	**48.000**

example, the rate of change for the headwater catchment with 20.5% wetland (c38) was 10 days per decade earlier for the 10th percentile ($P < 0.01$) of the spring discharge frequency distribution. In comparison, the significant rates of change for the headwater catchment with 1.1% wetland (c35) were primarily in the higher percentiles (i.e. 75th, 80th and 90th), including almost 10 days per decade earlier for the 90th percentile ($P < 0.01$) (Table IIB, Table IV). Furthermore, the number of days over which the majority of discharge flowed varied – in the headwater catchment with 20.5% wetland, discharge occurred over longer periods of time, while the duration decreased in the headwater catchment with 1.1% wetland (Table IV). Downstream of the headwater catchments, there were significant shift to earlier timing of discharge and increases in the duration (Table IV).

For the autumn frequency distribution of daily discharge that fell during the period from July to December (Table IV), percentiles generally occurred on a later day

Table III. Direction of slopes from Mann–Kendall and Theil–Sen analysis on precipitation data showing how the timing (shifts in the 10th, 20th, 25th, 50th, 75th, 80th and 90th percentiles) and duration (increases or decreases in the range of the 10th to 90th, 20th to 80th and 25th to 75th percentiles) of windows in the spring (January to June) and autumn (July to December) have changed between 1983 and 2009. Right arrows indicate a shift of the window to later in the year; left arrows indicate a shift to earlier in the year; down arrows indicate a narrowing of the window (more peaked frequency distribution); up arrows indicate a widening of the window (more flattened frequency distribution). Green cells indicate significance at $P < 0.05$, and blue cells indicate significance at $P < 0.1$

	Precipitation percentiles									
	Timing							Duration		
	10	20	25	50	75	80	90	10-90	20-80	25-75
Spring		←	→							
Autumn									↓	

Table IV. Direction of slopes from Mann–Kendall and Theil–Sen analysis on discharge data showing how the timing (shifts in the 10th, 20th, 25th, 50th, 75th, 80th and 90th percentiles) and duration (increases or decreases in the range of the 10th to 90th, 20th to 80th and 25th to 75th percentiles) of windows in the spring (January to June) and autumn (July to December) have changed between 1983 and 2009. (Refer to Table III caption for the explanation of arrows and colours)

	Discharge percentiles																				
	Timing														Duration						
	Spring							Autumn							Spring			Autumn			
	10	20	25	50	75	80	90	10	20	25	50	75	80	90	10-90	20-80	25-75	10-90	20-80	25-75	
c38	←							→	→			→	→	→	↑						
c35						←	←	→	→	→						↓	↓	↓	↓	↓		
s0									→										↓	↓	
s1	←								→					→					↓	↓	
s2														→							
s3							←							→							
s4		←				←										↑					
s5	←	←	←											→		↑					

of the year (i.e. right arrows) indicating a shift to a later start of autumn discharge. Patterns in daily discharge were similar between both headwater catchments, which showed all percentiles trending towards a later day of the year. For example, the rate of change for the headwater catchment with significant wetland was about 5 days later per decade for the 75th percentile ($P < 0.01$). This and the other significant shifts in c38 were observed during the later percentiles (75th, 80th and 90th). In comparison, the rate of change in autumn discharge for the headwater catchment with no significant wetland was 10 days per decade later for the 25th percentile ($P < 0.05$). This and the other significant shifts in c35 were observed during the earlier percentiles (10th, 20th and 25th). Furthermore, the number of days over which the majority of discharge flowed became shorter in c35 over the time series (Tables IIB, 4); for example, the range of the 25th–75th percentile decreased by 10 days per decade ($P < 0.05$). Downstream of the headwater catchments, there was a general autumn pattern of later timing shifts, and significant decreases were observed in duration in s0 and s1 (Table IV), respectively. In general, changes in the timing and duration of the frequency distribution of precipitation and discharge were weaker in spring and stronger in autumn, and downstream of the headwater catchments, the signals became weaker (Table IV).

DISCUSSION

Forest condition

Globally, forests are in decline, with widespread reductions in growth attributed to climate change (Allen *et al.*, 2010). While drought and heat stress due to climate change are major factors in suppressing tree growth and inducing mortality, other factors related to climate change (such as increases in the frequency and intensity of fires and insect outbreaks) act synergistically with these stressors to produce forest decline (Dale *et al.,* 2001; Mohan *et al.,* 2009). And while rising CO_2 may help

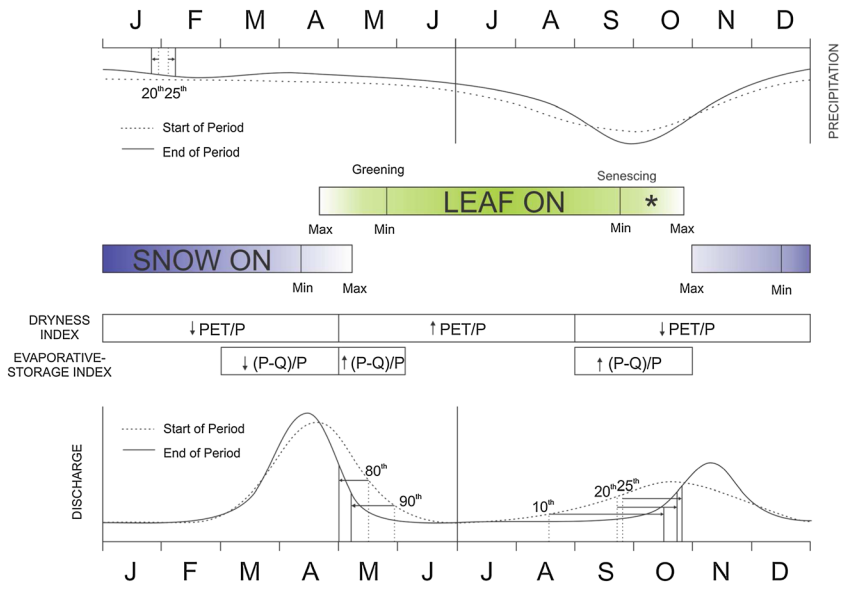

Figure 7. Conceptual diagram showing how catchment characteristics have changed over three decades based on trends in precipitation, phenology, snow cover, dryness and evaporative-storage indices, and discharge in the c35 catchment of the Turkey Lakes Watershed. There was natural variation in the timing of snow and canopy greening, but only the canopy senescing showed a significant trend towards delayed senescence in the autumn period. In the precipitation and discharge frequency distributions, the arrows indicate significant shifts in the timing of percentiles, and the change in peak size indicates changes in the ranges of the percentiles

offset future heat stress and drought in forests through its effects on photosynthetic heat tolerance and stomatal conductance, experiments show that trees can actually become more susceptible to drought under high CO_2 because of their greater canopy size (Warren *et al.,* 2011; Way 2011a). In northern forests in Canada, declines in tree productivity and increases in tree mortality linked to increasing drought have already been observed (Peng *et al.*, 2011). In this study, we suggest that climate warming is affecting the ecology and hydrology of the northern forests of the temperate forest biome. A conceptual model of our research findings is presented in Figure 7. In this conceptual model, we show that over the past 30 years the forested landscape is becoming warmer and drier but with no remarkable changes in the seasonality of temperature or precipitation.

The growing season is starting to show evidence of lengthening, but the widths of the vernal and autumnal windows that shoulder the growing season are not changing. The hydrological cycle is intensifying, particularly during the summer growing season, where PET/P is increasing during these months, and during the vernal and autumnal windows, where the discharge is becoming smaller and shifting earlier in spring and later in autumn from the growing season. This intensification of hydrological cycling during these windows is likely to have feedbacks that will influence the potential for summer forest growth. The lengthened growing season in this study was mostly driven by delayed leaf senescence, when photosynthetic activity is quite low in this high-latitude region (Bauerle *et al.*, 2012). Therefore, it may have a limited effect on forest growth compared with lengthened growing season driven by early greenup. Richardson *et al.* (2010) also reported that forest productivity was significantly correlated to the greenup timing rather than senescence from the FluxNet data of nine deciduous broadleaf forest, most of which are located at high latitudes (>40°N). In the temperate forests of the Great Lakes region, future forest growth is predicted to be most sensitive to climate changes resulting in a transition from temperature limitation to water limitation (Peters *et al.*, 2013), implying that the trends we document here are likely to lead to decreased forest growth, if they have not already.

Forest vernal and autumnal windows

Grime (1994) coined the term 'vernal window' in reference to the period of high light irradiance reaching the forest floor under an open forest canopy that creates an 'ecological opportunity' for enhanced growth (Tockner, 2010). The northern limits of the temperate forest biome are getting warmer, and this warming may result in a 'widening' of both the vernal and autumnal windows if temperature is a more important driver on the timing of snowpack dynamics than on canopy phenology. The notion of climate warming triggering a widening of this vernal window of ecological opportunities assumes that the ecosystem is temperature-limited, which is a reasonable assumption in higher latitude forests where cold temperatures generally delimit the growing season

and water is not limiting. However, we found that a mean temperature increase of 0.6 °C per decade has resulted in no evidence of a widening of either the vernal or autumnal windows, although we did find this warming has led to a slightly longer growing season, similar to other studies (e.g. Menzel *et al.*, 2006; Richardson *et al.*, 2006; Jeganathan *et al.*, 2014).

Intensification of hydrological cycling during these windows

Previous studies in the temperate forest biome have shown declines in surface flows over recent years. For example, in the TLW, Mengistu *et al.* (2013) observed climate warming in TLW of 0.7 °C per decade from 1981 to 2008, with a combination of signals that were stationary (55% = 0.37 °C) and non-stationary (45% = 0.30 °C related to the Atlantic Multidecadal Oscillation) [note that the different time series (1983–2009) used in this study resulted in a slightly lower rate of warming of 0.6 °C per decade]. The rate of decline in water yield was highest (−14.6 mm/year) in the catchment with lower water-loading and lower water-storage capacities (c35) ($r^2 = 0.52$, $P < 0.001$) and nearly as high (−13.0 mm/year) in the catchment with similar water loading but higher water-storage capacity (c38) ($r^2 = 0.44$, $P < 0.001$). In this study, we found that this decline is not uniform over seasons. Based on Budyko's (1974) indices, the 'dryness index' (PET/P) that indicates whether the system is becoming drier or wetter and the 'evaporative-storage index' [(P – Q) / P] that indicates whether the system is partitioning more water to evapotranspiration or discharge, we found evidence that (1) climate warming is leading to intensification of the hydrological cycle (indicated in the TLW by decreases in P and Q) or possibly changes in storage and (2) climate effects are asymmetric across the seasons, such that even though water fluxes are declining, autumn, winter and spring months are relatively wetter compared with the summer months. However, discharge during the vernal and autumnal windows is also shifting – becoming earlier in spring and later in autumn – and the frequency distributions are becoming more peaked in the autumn, so that the period of no to low flows may be increasing in the shoulder seasons. This intensification of the hydrological cycle may lead to a transformation of the traditional discharge hydrographs to smaller and potentially flashier (i.e. more peaked) discharges that occur earlier in spring and later in autumn.

Hydrological feedbacks on forest growth

One might assume that climate warming would equally alter both snowpack and canopy dynamics. However, our work indicates that forest hydrology appears to respond differently to temperature than canopy phenology. This difference in sensitivity to climate warming has important implications for forest ecosystems, because the greater temperature sensitivity of the hydrological cycle may uncouple spring hydrological dynamics from the physiological demands that set the trajectory for summer forest growth.

In other northern forests, declines in productivity and increases in mortality have been attributed to midsummer drying (Peng *et al.*, 2011). Specifically, earlier snowmelts have been linked to decreased productivity in the summers, because of lower soil water availability (Angert *et al.*, 2005; Hu *et al.*, 2010; Buermann *et al.*, 2013). Our data are consistent with this result. We observed not only declines in annual discharge but also changes in the monthly distribution of atmospheric drying potential (PET/P) with trends of higher PET/P in summer months and lower PET/P for all other months, and changes in the atmospheric drying potential have been found to be a more important driver of forest decline than temperature *per se* (Eamus *et al.* (2013). As water is often the main driver of inter-annual variability in forest productivity (e.g. Brummer *et al.*, 2012), an intensification of hydrological cycling driven by climate warming that leads to earlier spring snowmelts (i.e. earlier spring discharge and presumably less soil moisture to fuel the growing season) will likely lead to a reduction in forest productivity, and therefore may be an important factor contributing to the broad-scale declines in productivity in northern forests (Buermann *et al.*, 2013). Sugar maple dominated forests are expected to migrate approximately 1000 km north by 2071 to 2100 (McKenney *et al.*, 2007). Under this scenario, the Turkey Lakes Watershed would be situated in the middle of the forest's range, rather than the northern edge.

Furthermore, we observed delayed and more concentrated autumn discharge. It is possible that this delayed discharge is due to larger soil water deficits towards the late growing season, such that once the autumn storms arrive, there is a time lag for water tables to fill prior to any significant increase in discharge (Mengistu *et al.*, 2014). The concept of ecological opportunities existing within the vernal and autumnal windows needs to recognize the hydrological underpinnings of these windows. There are fundamental hydrological changes occurring within the vernal and autumnal windows. Those species that are able to respond to the new 'niches' created by warmer temperatures, especially in the vernal or autumnal windows, could develop a competitive advantage over other species. Therefore, the spring and autumn 'triggers' coupled with summer drying may speed up this positive feedback leading to faster declines in growth of the current dominant tree species.

Downstream effects

Alterations of forest hydrological flows may impact associated biogeochemical flows (the movement of nutrients), which are likely to have significant consequences for primary productivity of the terrestrial system and the primary productivity of downstream aquatic ecosystems. While we observed no change in the *terrestrial* vernal or autumnal windows (perhaps because of photoperiodic limitations of the dominant tree species) (Bauerle *et al*., 2012), there is evidence from other studies that supports a change in the *aquatic* vernal and autumnal windows (e.g. Winter *et al*., 2011), likely because of (1) alleviation of temperature limitations in surface waters and (2) more nutrient supplies from forested areas that can no longer take up the water and nutrients that are available during the vernal and autumnal windows. Fundamental changes are taking place in the primary productivity of aquatic ecosystems on forested landscapes. For example, algal blooms have significantly increased in nutrient-poor oligotrophic lakes within the temperate forest biome of Canada (Winter *et al*., 2011) and the USA (Carey *et al*., 2008) over the same time period as our climate-warming trajectory. These algal blooms both initiate and persist later in the autumn season (from September to November), corresponding to a delayed onset in timing and magnitude of autumnal storms. This increase in algal bloom reports is primarily comprised of potentially toxin-producing cyanobacteria (Winter *et al*., 2011). If autumn storms are shifting to the post-canopy leaf fall period, this will have significant consequences for nutrient loading to the warmer lakes. The increased temperatures prolong the period of opportunity for algal growth, and the shift in timing of autumn discharge that now flows through freshly fallen leaf litter delivering a fresh supply of nutrients to aquatic ecosystems, may give cyanobacteria a competitive advantage (Creed *et al.*, 2013) that leads to a greater number of cyanobacteria algal blooms occurring later in the year (Winter *et al.*, 2011).

Future work

We conducted this study on the northern limit of the temperate forest of North America. The rates of climate warming, combined with changes in precipitation and discharge patterns, are likely to vary throughout the temperate forest biome. Future research activities will apply a similar approach and explore the effects of an 'intensification' of hydrological cycling on different tree species located in warmer, more southern temperate forests. Furthermore, future research activities will explore the effects of changes in the timing and magnitude of hydrological and associated biogeochemical discharge on the productivity of the coupled terrestrial-aquatic ecosystem.

CONCLUSION

A 0.6 °C per decade climate warming over the past 27 years has occurred in a northern forest of the temperate biome of eastern North America. There were no strong monthly trends in temperature, but the effects of this overall warming had a seasonality characterized by a relatively drier growing season, and a relatively wetter dormant season. There was evidence that the ecological opportunity created by vernal and autumnal windows (which are important for setting the trajectory of forest growth) may be starting to change, as a modest extension of the length of the growing season was observed in recent years. There was also evidence for an alteration of hydrological flows, specifically, climate warming lead to an intensification of the hydrological cycle, with a greater atmospheric drying potential during the summer growing season, and smaller, more concentrated (autumn only) discharges occurring earlier in the spring and later in the autumn. The shift in the timing and duration of hydrological flows away from the growing season, coupled with greater partitioning of water to evapotranspiration than discharge during the growing season, may be an important factor contributing to recent declines in the productivity of northern forests.

ACKNOWLEDGEMENTS

We acknowledge NWRI for meteorology and GLFC and NWRI for discharge data for headwater streams (F. D. Beall, GLFC), stream water discharge over the chain of lakes (D. S. Jeffries, NWRI) and snow cover data (R. G. Semkin, Environment Canada). This study was supported by NSERC Discovery grants to I. F. C. and D. A. W. and the NSERC Canadian Network for Aquatic Ecosystem Services.

REFERENCES

Allen CD, Macalady AK, Chenchouni H, Bachelet D, McDowell N, Vennetier M, Kitzberger T, Rigling A, Breshears DD, Hogg EH (Ted), Gonzalez P, Fensham R, Zhang Z, Castro J, Demidova N, Lim J-H, Allard G, Running SW, Semerci A, Cobb N. 2010. A global overview of drought and heat-induced tree mortality reveals emerging climate change risks for forests. *Forest Ecology and Management* **259**: 660–684.

Angert A, Biraud S, Bonfils C, Henning CC, Buermann W, Pinzon J, Tucker CJ, Fung I. 2005. Drier summers cancel out the CO_2 uptake enhancement induced by warmer springs. *Proceedings of the National Academy of Sciences of the United States of America* **102**: 10823–10827.

Bauerle WL, Oren R, Way DA, Qian SS, Stoy PC, Thornton PE, Bowden JD, Hoffman FM, Reynolds RF. 2012. Photoperiodic regulation of the seasonal pattern of photosynthetic capacity and the implications for carbon cycling. *Proceedings of the National Academy of Sciences of the United States of America* **109**: 8612–8617.

Beniston M, Stephenson DB, Christensen OB, Ferro CAT, Frei C, Goyette S, Halsnaes K, Holt T, Jylhä K, Koffi B, Palutikof J, Schöll R, Semmler T,

Woth K. 2007. Future extreme events in European climate: an exploration of regional climate model projections. *Climatic Change* **81**: 71–95.

Boisvenue C, Running SW. 2006. Impacts of climate change on natural forest productivity–evidence since the middle of the 20th century. *Global Change Biology* **12**: 862–882.

Brodzik M, Armstrong R. 2013. *Northern Hemisphere EASE-Grid 2.0 Weekly Snow Cover and Sea Ice Extent. Version 4*. NASA DAAC at the National Snow and Ice Data Center: Boulder, Colorado USA.

Brümmer C, Black TA, Jassal RS, Grant NJ, Spittlehouse DL, Chen B, Nesic Z, Amiro BD, Arain MA, Barr AG, Bourque CP-A, Coursolle C, Dunn AL, Flanagan LB, Humphreys ER, Lafleur PM, Margolis HA, McCaughey JH, Wofsy SC. 2012. How climate and vegetation type influence evapotranspiration and water use efficiency in Canadian forest, peatland and grassland ecosystems. *Agricultural and Forest Meteorology* **153**: 14–30.

Budyko MI. 1974. *Climate and Life*. Academic Press: New York; 508.

Buermann W, Bikash PR, Jung M, Burn DH, Reichstein M. 2013. Earlier springs decrease peak summer productivity in North American boreal forests. *Environmental Research Letters* **8**: 024027.

Capell R, Tetzlaff D, Essery R, Soulsby C. 2014. Projecting climate change impacts on stream flow regimes with tracer-aided runoff models – preliminary assessment of heterogeneity at the mesoscale. *Hydrological Processes* **28**: 545–558.

Carey CC, Weathers KC, Cottingham KL. 2008. *Gloeotrichia echinulata* blooms in an oligotrophic lake: helpful insights from eutrophic lakes. *Journal of Plankton Research* **30**: 893–904.

Carroll ML, DiMiceli CM, Sohlberg RA, Townshend JRG. 2006. *250 m MODIS Normalized Difference Vegetation Index, Collection 4*. University of Maryland: College Park, Maryland.

Chou C, Neelin JD, Chen C-A, Tu J-Y. 2009. Evaluating the "Rich-Get-Richer" mechanism in tropical precipitation change under global warming. *Journal of Climate* **22**: 1982–2005.

Cleveland RB, Cleveland WS, McRae JE, Terpenning I. 1990. STL: a seasonal-trend decomposition procedure based on loess. *Journal of Official Statistics* **6**: 3–73.

Cowan IR, Farquhar GD. 1977. Stomatal function in relation to leaf metabolism and environment. In: *Integration of Activity in the Higher Plant*, Jennings DH (ed). Cambridge Univ. Press: Cambridge; 471–505.

Craig D, Johnston L. 1988. Acidification of shallow groundwaters during the spring melt period. *Nordic Hydrology* **19**: 89–98.

Creed IF, Beall FD. 2009. Distributed topographic indicators for predicting nitrogen export from headwater catchments. *Water Resources Research* **45**: W10407.

Creed IF, Mengistu SG, Lutz B. 2013. *What do Spatio-Temporal Signals in Stream Nutrient Export from Naturally Forested Landscapes Teach us About Catchment Form and Function? American Geophysical Union Fall Meeting, December 9–13*. CA: San Francisco.

Creed IF, Spargo AT, Jones JA, Buttle JM, Adams MB, Beall FD, Booth EG, Campbell JL, Clow D, Elder K, Green MB, Grimm NB, Miniat C, Ramlal P, Saha A, Sebestyen S, Spittlehouse D, Sterling S, Williams MW, Winkler R, Yao H. 2014. Changing forest water yields in response to climate warming: results from long-term experimental watershed sites across North America. *Global Change Biology* **20**: 3191–3208.

Creed IF, Trick CG, Band LE, Morrison IK. 2002. Characterizing the spatial pattern of soil carbon and nitrogen pools in the Turkey Lakes Watershed: a comparison of regression techniques. *Water, Air, and Soil Pollution: Focus* **2**: 81–102.

Dale VH, Joyce LA, McNulty S, Neilson RP, Ayres MP, Flannigan MD, Hanson PJ, Irland LC, Lugo AE, Peterson CJ, Simberloff D, Swanson FJ, Stocks BJ, Wotton BM. 2001. Climate change and forest disturbances. *BioScience* **51**: 723–734.

Durack PJ, Wijffels SE, Matear RJ. 2012. Ocean salinities reveal strong global water cycle intensification during 1950 to 2000. *Science* **335**: 455–458.

Eamus D, Boulain N, Cleverly J, Breshears DD. 2013. Global change-type drought-induced tree mortality: vapor pressure deficit is more important than temperature per se in causing decline in tree health. *Ecology and Evolution* **3**: 2711–2729.

Elliot H. 1985. Geophysical survey to determine overburden thickness in selected areas within the Turkey Lakes Watershed basin, Algoma District, Ontario. Rep. 85-09, Turkey Lakes Watershed, Algoma, Ontario, Canada.

Environment Canada. 2014. HYDAT database: surface water and sediment data to 2014, Water Survey of Canada. Accessed January 21, 2014, http://www.ec.gc.ca/rhc-wsc/

Fisher JI, Mustard JF, Vadeboncoeur MA. 2006. Green leaf phenology at landsat resolution: scaling from the field to the satellite. *Remote Sensing of Environment* **100**: 265–279.

Grime JP. 1994. The role of plasticity in exploiting environmental heterogeneity. In *Exploitation of Environmental Heterogeneity by Plants: Ecophysiological Processes Above- and Belowground*, Caldwell MM, Pearcy RW (Eds). Academic Press: San Diego; 1–19.

Hamon WR. 1963. Computation of direct runoff amounts from storm rainfall. *International Association of Scientific Hydrological Publications* **63**: 52–62.

Hu J, Moore DJP, Burns SP, Monson RK. 2010. Longer growing seasons lead to less carbon sequestration in a subalpine forest. *Global Change Biology* **16**: 771–783.

Hwang T, Band LE, Miniat CF, Song C, Bolstad PV, Vose JM, Love JP. 2014. Divergent phenological response to hydroclimate variability in forested mountain watersheds. *Global Change Biology* **20**: 2580–2595.

Hwang T, Song C, Bolstad P, Band LE. 2011b. Downscaling real-time vegetation dynamics by fusing multi-temporal MODIS and Landsat NDVI in topographically complex terrain. *Remote Sensing of Environment* **115**: 2499–2512.

Hwang T, Song C, Vose JM, Band LE. 2011a. Topography-mediated controls on local vegetation phenology estimated from MODIS vegetation index. *Landscape Ecology* **26**: 541–556.

Jansen E, Overpeck J. 2007. Palaeoclimate. In *Climate Change 2007: The Physical Science Basis. Contribution of Working Group I to the Fourth Assessment Report of the Intergovernmental Panel on Climate Change*, Solomon S, Qin D, Manning M, et al (Eds). Cambridge University Press: Cambridge, United Kingdom and New York, NY, USA; 433–497.

Jeffries DS, Kelso J, Morrison IK. 1988. Physical, chemical and biological characteristics of the Turkey Lakes watershed, central Ontario, Canada. *Canadian Journal of Fisheries and Aquatic Sciences* **45**(1): 3–13.

Jeganathan C, Dash J, Atkinson PM. 2014. Remotely sensed trends in the phenology of high latitudinal vegetation, controlling for land cover change and vegetation type. *Remote Sensing of the Environment* **143**: 154–170.

Jenson SK, Domingue JO. 1988. Extracting topographic structure from digital elevation data for geographic information system analysis. *Photogrammetric Engineering & Remote Sensing* **54**: 1593–1600.

Jones JA, Creed IF, Hatcher KL, Warren RJ, Adams MB, Benson MH, Boose E, Brown WA, Campbell JL, Covich A, Clow DW, Dahm CN, Elder K, Ford CR, Grimm NB, Henshaw DL, Larson KL, Miles ES, Miles KM, Sebestyen SD, Spargo AT, Stone AB, Vose JM, Williams MW. 2012. Ecosystem processes and human influences regulate discharge response to climate change at long-term ecological research sites. *BioScience:* **62**: 390–404.

Katz RW, Brown BG. 1992. Extreme events in a changing climate: variability is more important than averages. *Climatic Change* **21**: 289–302.

Lehner B, Döll P, Alcamo J, Henrichs T, Kaspar F. 2006. Estimating the impact of global change on flood and drought risks in Europe: a continental, integrated analysis. *Climatic Change* **75**: 273–299.

Lindsay JB, Creed IF. 2005. Removal of artifact depressions from digital elevation models: towards a minimum impact approach. *Hydrological Processes* **19**: 3113–3126.

Lu J, Sun G, McNulty SG, Amatya DM. 2005. A comparison of six potential evapotranspiration methods for regional use in the southeastern United States. *Journal of the American Water Resources Association* **41**: 621–633.

Marquardt DW. 1963. An algorithm for least-squares estimation of nonlinear parameters. *Journal of the Society for Industrial and Applied Mathematics* **11**: 431–441.

McKenney DW, Pedlar JH, Lawrence K, Campbell K, Hutchinson MF. 2007. Potential impacts of climate change on the distribution of North American trees. *BioScience* **57**: 939–948.

Mengistu SG, Creed IF, Kulperger RJ, Quick CG. 2013. Russian nesting dolls effect – Using wavelet analysis to reveal non-stationary and nested

stationary signals in water yield from catchments on a northern forested landscape. *Hydrological Processes* **27**: 669–686.

Mengistu SG, Creed IF, Webster KL, Enanga E, Beall FD. 2014. Searching for similarity in topographic controls on carbon, nitrogen and phosphorus export from forested headwater catchments. *Hydrological Processes* **28**: 3201–3216.

Menzel A, Sparks TH, Estrella N, Koch E, Aasa A, Ahas R, Alm-Kübler R, Bissolli P, Braslavská O, Briede A, Chmielewsk FM, Crepinsek Z, Curnel Y, Dahl Å, Defila C, Donnelly A, Filella Y, Jatczak K, Måge F, Mestre A, Nordli Ø, Peñuelas J, Pirinen P, Remišová V, Scheifinger H, Striz M, Susnik A, Van Vliet AJH, Wielgolaski F-E, Zach S, Zust A. 2006. European phenological response to climate change matches the warming pattern. *Global Change Biology* **12**: 1969–1976.

Mohan JE, Cox RM, Iverson LR. 2009. Composition and carbon dynamics of forests in northeastern North America in a future, warmer world. *Canadian Journal of Forest Research* **39**: 213–230.

Morisette JT, Richardson AD, Knapp AK, Fisher JI, Graham EA, Abatzoglou J, Wilson BE, Breshears DD, Henebry GM, Hanes JM, Liang L. 2008. Tracking the rhythm of the seasons in the face of global change: phenological research in the 21st century. *Frontiers in Ecology and the Environment* **7**: 253–260.

O'Callaghan JF, Mark DM. 1984. The extraction of drainage networks from digital elevation data. *Computer Vision Graphics Image Processing* **28**: 323–344.

Peters EB, Wythers KR, Zhang S, Bradford JB, Reich PB. 2013. Potential climate change impacts on temperate forest ecosystems. *Canadian Journal of Forest Research* **43**: 939–950.

Peng C, Ma Z, Lei X, Zhu Q, Chen H, Wang W, Liu S, Li W, Fang X, Zhou X. 2011. A drought-induced pervasive increase in tree mortality across Canada's boreal forests. *Nature Climate Change* **1**: 467–471.

Planchon O, Darboux F. 2001. A fast, simple and versatile algorithm to fill the depressions of digital elevation models. *Catena* **46**: 159–176.

Richardson AD, Black TA, Ciais P, Delbart N, Friedl MA, Gobron N, Hollinger DY, Kutsch WL, Longdoz B, Luyssaert S, Migliavacca M, Montagnani L, Williammunger J, Moors E, Piao S, Rebmann C, Reichstein M, Saigusa N, Tomelleri E, Vargas R, Varlagin A. 2010. Influence of spring and autumn phenological transitions on forest ecosystem productivity. *Philosophical Transactions of the Royal Society B-Biological Sciences* **365**: 3227–3246.

Richardson AD, Schenk Bailey A, Denny EG, Martin CW, O'keefe J. 2006. Phenology of a northern hardwood forest canopy. *Global Change Biology* **12**: 1174–1188.

Rouse JW, Haas RS, Schell JA, Deering DW. 1973. Monitoring vegetation systems in the Great Plains with ERTS. Proceedings, 3rd ERT S Symposium **1**: 309–317.

Rustad L, Campbell J, Dukes JS, Huntington T, Fallon Lambert K, Mohan J, Rodenhouse N. 2012. Changing climate, changing forests: the impacts of climate change on forests of the northeastern United States and eastern Canada. *U.S. Forest Service General Technical Report* **NRS-99**: 48pp.

Semkin RG, Jeffries DS. 1983. Rock chemistry in the Turkey Lakes Watershed. *Turkey Lakes Watershed Unpublished Report; No.* **83**(03): 9.

Sen PK. 1968. Estimates of the regression coefficient based on Kendall's tau. *Journal of the American Statistical Association* **63**: 1379–1389.

Stoy PC, Trowbridge AM, Bauerle WL. 2014. Controls on seasonal patterns of maximum ecosystem carbon uptake and canopy-scale photosynthetic light response: contributions form both temperature and photoperiod. *Photosynthesis Research* **119**: 49–64.

Tockner K, Pusch M, Borchardt D, Lorang MS. 2010. Multiple stressors in coupled river – floodplain ecosystems. *Freshwater Biology* **55**: 135–151.

Tucker CJ, Pinzon JE, Brown ME, Slayback DA, Pak EW, Mahoney R, Vermote EF, El Saleous N. 2005. An extended AVHRR 8-km NDVI data- set compatible with MODIS and SPOT vegetation NDVI data. *International Journal of Remote Sensing* **26**: 4485–4498.

Warren JM, Norby RJ, Wullschleger SD. 2011. Elevated CO_2 enhances leaf senescence during extreme drought in a temperate forest. *Tree Physiology* **31**: 117–130.

Way DA. 2011a. The bigger they are, the harder they fall: CO_2 concentration and tree size affect drought tolerance. *Tree Physiology* **31**: 115–116.

Way DA. 2011b. Tree phenology responses to warming: spring forward, fall back? *Tree Physiology* **31**: 469–471.

Wickware GM, Cowell DW. 1985. Forest ecosystem classification of the Turkey Lake Watershed, ecology. Classif. Ser. 18, Lands Dir., Environ, Ottawa, Canada.

Winter JG, DeSellas AM, Fletcher R, Heintsch L, Morley A, Nakamoto L, Utsumi K. 2011. Algal blooms in Ontario, Canada: increases in reports since 1994. *Lake and Reservoir Management* **27**: 105–112.

Yue S, Pilon P, Cavadias G. 2002. Power of the Mann–Kendall and Spearman's rho tests for detecting monotonic trends in hydrological series. *Journal of Hydrology* **259**: 254–271.

Zhang X, Friedl MA, Schaaf CB, Strahler AH. 2004. Climate controls on vegetation phonological patterns in northern mid- and high latitudes inferred from MODIS data. *Global Change Biology* **10**(7): 1133–1145.

Zhang X, Tarpley D, Sullivan JT. 2007. Diverse responses of vegetation phenology to a warming climate. *Geophysical Research Letters* **34**: L19405.

Zhang X, Vincent LA, Hogg WD, Niitsoo A. 2000. Temperature and precipitation trends in Canada during the 20th century. *Atmosphere-Ocean* **38**: 395–429.

Zhu Z, Bi J, Pan Y, Ganguly S, Anav A, Xu L, Samanta A, Piao S, Nemani RR, Myneni RB. 2013. Global data sets of vegetation leaf area index (LAI) 3 g and Fraction of Photosynthetically Active Radiation (FPAR) 3 g derived from Global Inventory Modeling and Mapping Studies (GIMMS) Normalized Difference Vegetation Index (NDVI3g) for the period 1981 to 2011. *Remote Sensing* **5**: 927–948.